A totally asymmetric exclusion process with stochastically mediated entrance and exit

2009 J. Phys. A: Math. Theor. 42 445002

(http://iopscience.iop.org/1751-8121/42/44/445002)

IOP PUBLISHING JOURNAL OF PHYSICS A: MATHEMATICAL AND THEORETICAL

J. Phys. A: Math. Theor. **42** (2009) 445002 (10pp) doi:10.1088/1751-8113/42/44/445002

A totally asymmetric exclusion process with stochastically mediated entrance and exit

A Jamie Wood

York Centre for Complex Systems Analysis, Departments of Mathematics and Biology, University of York, York, YO10 5YW, UK

E-mail: ajw511@york.ac.uk

Received 8 July 2009, in final form 10 September 2009
Published 8 October 2009
Online at stacks.iop.org/JPhysA/42/445002

Abstract

The asymmetric exclusion process is a well-established model in statistical physics that exhibits non-equilibrium phase transitions. It has received considerable attention of late as it is widely applicable to problems in molecular biology involving the transit of component parts along specified tracks or pathways. In this paper we use a self-consistent mean-field approach, backed up by Monte Carlo simulations, to examine the case where the exit from such a track is 'gated' by the presence of some external component that is capable of binding and unbinding from an additional site to the track; exit from the path is only possible by the bound presence of this component. We not only compute the relevant phase diagrams for this instance both in terms of the exit and entrance rates but also the binding and unbinding rates of the 'gate' and comment on this model's applicability to problems in biology.

PACS numbers: 05.40.−a, 87.15.a, 87.15.hj

1. Introduction

The asymmetric exclusion process has become a ubiquitous theoretical substrate for examining non-equilibrium transport problems in biology. Applications have included tracked molecular motors [1], protein kinetics [2] and fungal hyphae [4]. There is now a substantive body of existing work that details the different phases of the model, reviewed recently [5], with additional rigour provided by exact calculations performed nearly 15 years ago [6]. Of particular interest for this paper is the well-established self-consistent mean-field approach [7, 8] that allows the exact results to be leveraged to provide solutions in both heterogeneous and compound configurations. This approach was originally introduced for defects with the chain [8–10], but has subsequently been used for combining symmetric exclusion processes (diffusive-like) in series [11] and in parallel [12, 13].

Whilst transport is the focus of these models, of equal interest to applications in molecular biology, for example, are reactions at the entrance and terminus of channels that obey

asymmetric exclusion dynamics. Ultimately, in applications in this area it is the interactions occurring as a *consequence* of transport, for example as in the hyphae growth case [4], that will determine the effectiveness and realism of the modelling approach. To this end we imagine a situation where the channel is transporting a useful particle or packet to an end point where a receptor is potentially awaiting which will transport the particle to some further function. Rather than assuming regular periodic conditions [14] we assume that a fixed pool of receptors bind on and bind off the terminus with some prescribed rate. If a receptor is successfully bound, then a particle may exit the track accompanied by the receptor. We also consider the case where similar dynamics occur at the entrance to the channel; as well as the most general situation where both operate simultaneously. A related effect is where instead of transporting the incoming or outgoing particles, the receptor or initiator only mediates the exit or entrance; in effect the particles are simply diffusable input or output nozzles for the non-equilibrium track. For example, input nozzles would be an apt approximation for sigma factors, if the TASEP was representing bacterial transcription.

In this paper we address these simple gating effects, and show how they impact on the dynamics of the channel. We first describe our models and then show self-consistent mean-field calculations for the resultant phases. We then present our modelling results and compare them to theory, highlighting where, and the manner in which, the simple MF calculation breaks down. Finally, we summarize our findings and suggest some additional extensions and applications.

2. The model

We consider a linear system consisting of L sites, indexed by $i = 1, 2, \ldots, L$, within which particles are able to hop in single rightward steps through the system. Exclusion dynamics apply, so hops are only permitted if the subsequent site is empty. We take the inter-site hops to set the timescale in the model, so they hop at rate 1. Particles are injected into the system at the left-hand edge with rate α if site 1 is vacant and are removed with rate β if site L is occupied. This system describes the standard TASEP model for which an exact solution is known [6] and has three distinct phases: a max current (MC) phase, a low-density (LD) phase and a high-density (HD) phase. These are defined by the current (J), the bulk density, l_{bulk}, and the densities at the beginning (l_1) and end (l_L). The results can be mathematically summarized [5, 6, 8] as follows: where $\alpha \geqslant \frac{1}{2}$ and $\beta \geqslant \frac{1}{2}$ then the system is MC with

$$J = \frac{1}{4}, \qquad l_1 = 1 - \frac{1}{4\alpha}, \qquad l_L = \frac{1}{4\beta}, \qquad l_{\text{bulk}} = \frac{1}{2}; \tag{1}$$

where $\alpha < \frac{1}{2}$ and $\beta \geqslant \alpha$ the bulk properties are dictated by the entrance conditions and the system is LD with

$$J = \alpha(1-\alpha), \qquad l_1 = \alpha, \qquad l_L = \frac{\alpha(1-\alpha)}{\beta}, \qquad l_{\text{bulk}} = \alpha; \tag{2}$$

where $\beta < \frac{1}{2}$ and $\alpha \geqslant \beta$ the bulk properties are dictated by the exit conditions and the system is HD with

$$J = \beta(1-\beta), \qquad l_1 = 1 - \frac{\beta(1-\beta)}{\alpha}, \qquad l_L = 1-\beta, \qquad l_{\text{bulk}} = 1-\beta, \tag{3}$$

which together give the well-known phase diagram with second-order transitions between MC and the other two phases and a first-order transition between the LD and HD phases.

The self-consistent mean-field approach, introduced by [7], is able to leverage non-exact, but internally consistent solutions in more complex situations by assuming the differing

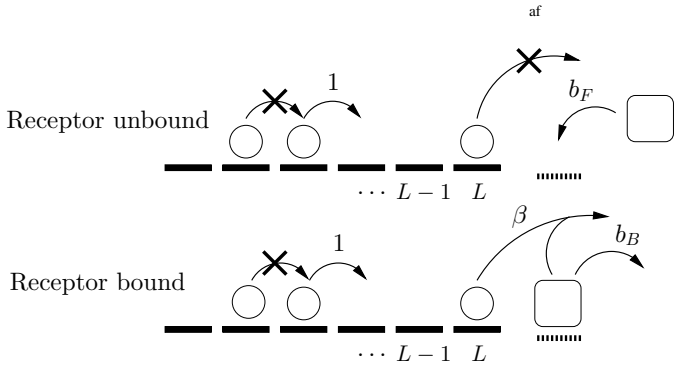

Figure 1. A simple diagrammatic representation of the entrance gate on a TASEP system. The possible processes that could occur in particular configuration when the gate is closed (upper) or open (lower). Note that if site L were unoccupied, then the process of simultaneous binding and detachment from the gate site with rate β would no longer be possible and instead the dynamics of the receptor binding would continue independently.

possible configurations of the trackway and the requisite conditions and then seeking contradictions or algebraic solutions dependent on the boundary conditions. This method is elegant and demonstrates the power of an exact solution; its weakness is that it ignores possible correlations from boundary conditions or internal defects that may project into the bulk sufficiently to alter the phase diagram. This of course is more prevalent close to transition boundaries where correlation lengths diverge. Of particular interest is how this method can be used to link together different TASEP trackways such that the interactions between them determine the bulk properties; this is implicitly the manner in which the defect site works as the defect site provides the link between the two halves of the track [8].

The novel feature of the model we consider is the addition of binding and unbinding of separate components, which we call the receptor if binding to the end of the track and the initiator if binding to the beginning of the track, that mediate the exit and entrance of the particles on the track. The additional components bind to separate, off-lattice, sites, the occupation of which we denote χ_a at the entrance and χ_b at the exit. When a receptor (initiator) is bound to the terminating (starting) gate, site particles are able to exit (enter) as in the regular TASEP. The dynamics of this binding are as follows: the exit gate opens with rate b_F as a receptor binds and closes with rate b_B as it unbinds. If the gate is 'open', that is with a receptor bound to it, the particles at site L, if present, leave the system with rate β. Crucially the receptor also unbinds on this event—the particles close the gate behind them—motivated by the receptor now performing some task with the particle that is has now gained. In summary

- $10 \to 01$ with rate 1
- $0 \to 1$ at site 1 with rate α
- $\emptyset$ (off lattice) $\rightleftharpoons \chi_b$ (off lattice) with rates b_F and b_B
- $\chi \to \emptyset$ (off lattice), $1 \to 0$ at site L with rate β.

This model is depicted diagrammatically in figure 1. The entrance gate operates in a similar fashion but with rates a_F and a_B and the particle enters the system with rate α, subject to a vacancy at site 1. It also unbinds when the particle enters the system. The simpler case of the diffusable nozzles follows an identical scheme to that described above, but now the off-lattice reaction ($\chi \to \emptyset$) no longer occurs in tandem with exit.

3. Theoretical analysis

3.1. Gated exit only

We analyse the model described above using self-consistent mean-field theory [8]. The first example consists of where the system is fed with a constant driving rate α and the exit is gated as described above. The behaviour of the average occupation of the gate $\langle\chi_b\rangle$ can be expressed simply as

$$\frac{\mathrm{d}\langle\chi_b\rangle}{\mathrm{d}t} = (1-\langle\chi_b\rangle)b_F - \langle\chi_b\rangle(b_B+\beta l_L) \tag{4}$$

and therefore at steady state we have

$$\langle\chi_b\rangle = \frac{b_F}{b_F+b_B+\beta l_L} \tag{5}$$

where we are assuming that correlations from this process do not impact on the system; we shall return to this later. In the slightly simpler case of the binding and unbinding exit nozzles, the exit condition is uncorrelated with the bulk and the βl_L term is dropped. This leads to a simple rescaling of the exit rate at steady state $\left(\beta \mapsto \beta\frac{b_F}{b_F+b_B}\right)$. However, this model has an identical description in terms of improved mean-field theory at the next order (described below) as to our main system of interest which implies that correlations induced by the exit conditions are identical.

The analysis now proceeds by assuming each of the different phases in turn for the model with an exit rate of $\beta\langle\chi_b\rangle$ which results in an equation that must be solved for $\langle\chi_b\rangle$. For simplicity we now drop the angle bracket notation in our expressions for χ_b (and later χ_a) except where explicitly indicated. We find that where $\alpha \geqslant \frac{1}{2}$, $\beta \geqslant \frac{1}{2}+\frac{2b_B+\frac{1}{2}}{4b_F-1}$ and $b_F > \frac{1}{4}$ the system is MC

$$J=\frac{1}{4} \qquad l_1 = 1-\frac{1}{4\alpha} \qquad l_L = \frac{b_F+b_B}{\beta(4b_F-1)} \qquad l_{\mathrm{bulk}} = \frac{1}{2} \qquad \chi_b = \frac{b_F-\frac{1}{4}}{b_F+b_B}; \tag{6}$$

where $\alpha < \frac{1}{2}$, $\beta > \frac{\alpha(b_F+b_B)}{b_F-\alpha(1-\alpha)}$ and $b_F > \alpha(1-\alpha)$ the system is LD with

$$J=\alpha(1-\alpha) \qquad l_1=\alpha \qquad l_L = \frac{\alpha(1-\alpha)(b_F+b_B)}{\beta(b_F-\alpha(1-\alpha))} \qquad l_{\mathrm{bulk}}=\alpha \qquad \chi_b = \frac{b_F-\alpha(1-\alpha)}{b_F+b_B} \tag{7}$$

and where $\beta < \frac{\alpha(b_F+b_B)}{b_F-\alpha(1-\alpha)}$, $\beta < \frac{1}{2}+\frac{2b_B+\frac{1}{2}}{4b_F-1}$ and $b_F > \frac{1}{4}$ the system is HD with

$$\begin{aligned}
J &= b_F + \frac{b_F+b_B}{2\beta^2}\left(\sqrt{(b_F+b_B+\beta)^2-4b_F\beta^2}-(b_F+b_B+\beta)\right)\\
l_1 &= 1-\frac{b_F}{\alpha}+\frac{b_F+b_B}{2\alpha\beta^2}\left(\sqrt{(b_F+b_B+\beta)^2-4b_F\beta^2}-(b_F+b_B+\beta)\right)\\
l_L &= \frac{1}{2}-\frac{b_F+b_B}{2\beta}+\frac{1}{2\beta}\sqrt{(b_F+b_B+\beta)^2-4b_F\beta^2}\\
l_{\mathrm{bulk}} &= \frac{1}{2}-\frac{b_F+b_B}{2\beta}+\frac{1}{2\beta}\sqrt{(b_F+b_B+\beta)^2-4b_F\beta^2}\\
\chi_b &= \frac{b_F-\alpha(1-\alpha)}{b_F+b_B}.
\end{aligned} \tag{8}$$

These analytic results are used to construct the solid lines for specific cases in both figure 2 and figure 3.

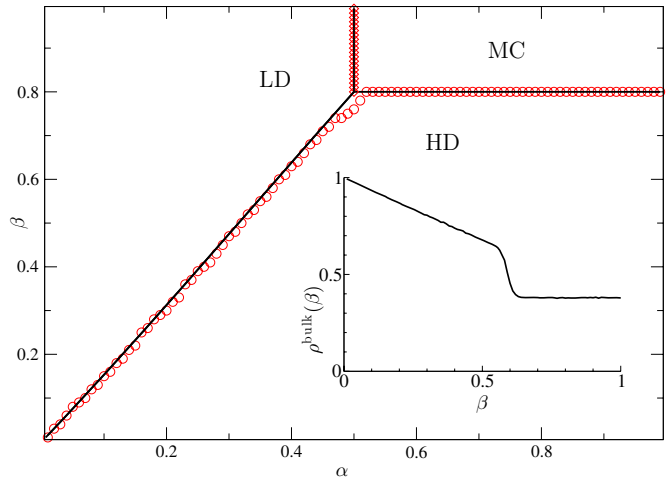

Figure 2. Phase portrait (left) for $L = 300$. Exit conditions are $b_F = 4.0$ and $b_B = 2.0$; entrance is a standard TASEP. Solid lines indicate the analytically computed phase boundaries ((6)–(8)). The circles indicate where a discontinuity was fitted from plots of $\rho(\beta)$, α fixed, diamonds where the dependences are reversed. A sample plot is shown of $\rho(\beta)$, $\alpha = 0.38$, comparing the predicted and simulated curves.

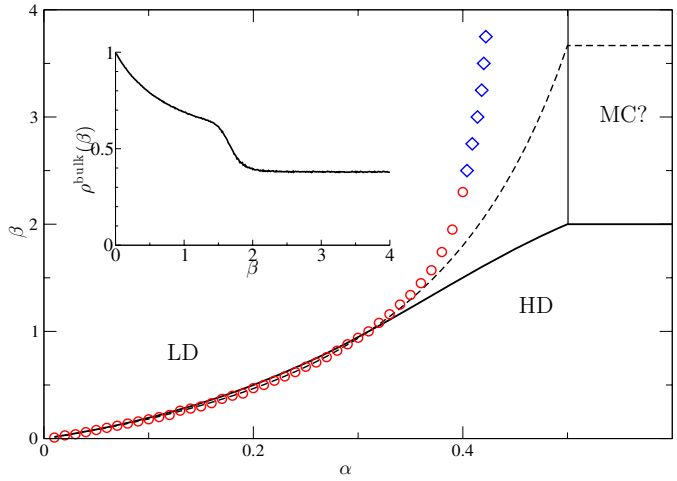

Figure 3. Phase portrait for $L = 300$. Exit conditions are $b_F = 0.4$ and $b_B = 0.2$; entrance is a standard TASEP. Once more a sample plot is shown of $\rho(\beta)$, $\alpha = 0.38$, comparing the predicted and simulated curves. The simulation results are shown as red circles (computationally fitted) and blue diamonds (fitted by hand). The normal theoretical predictions ((6)–(8)) are shown with a solid line and the improved mean-field predictions ((12)–(14)) are shown with a dashed line. It is clear that the results correspond to the predictions for low alpha, but as alpha increases the improved MF results fit the curve better. Then as alpha increases still further the simulation results diverge once more. The implication is that the system is unable to sustain a maximal current phase as correlations into the bulk increase with importance. The simulation results support the boundary asymptoting at $\approx \alpha = 0.43$.

(This figure is in colour only in the electronic version)

We anticipate that there will be significant deviations from these mean-field results where correlations of the exit site with the track become important and penetrate into the bulk. We can confirm this by systematically including the effects of including these correlations back into the system from the exit site using an improved version of the self-consistent mean-field theory previously used by Sugden and Evans in a system with similar complications [10, 15]. We perform this calculation by considering our TASEP system to run from site 1 to site $L-1$ and treat the last site, along with the exit site and the correlation between the two separately. The equations for the occupation of the gate site and the last track site are

$$\frac{\mathrm{d}\langle\chi_b\rangle}{\mathrm{d}t} = (1-\langle\chi_b\rangle)b_F - \langle\chi_b\rangle(b_B+\beta l_L) \tag{9}$$

$$\frac{\mathrm{d}\langle l_L\rangle}{\mathrm{d}t} = \langle l_{N-1}(1-l_N)\rangle - \beta\langle l_L\chi_b\rangle \tag{10}$$

respectively and the equation for the correlation between the last site and the receptor site can be found by considering possible reactions into and out of the state when both sites are occupied:

$$\frac{\mathrm{d}\langle l_L\chi_b\rangle}{\mathrm{d}t} = \langle l_{N-1}(1-l_N)\chi_b\rangle + b_F\langle l_N(1-\chi_b)\rangle - b_B\langle l_L\chi_b\rangle - \beta\langle l_L\chi_b\rangle. \tag{11}$$

The remainder of the trackway will now be in a max current phase if $1-l_L \geqslant \frac{1}{2}, \alpha \geqslant \frac{1}{2}$, and then $\langle l_{N-1}(1-l_N)\rangle = \langle l_{N-1}\rangle(1-\langle l_N\rangle) = \frac{1}{4}$. The average occupation of the gate site is unchanged and is given by (6) but now the equation for the occupation of $\langle l_L\rangle$ is quadratic. From this we can deduce that the max current phase is present when

$$\alpha \geqslant \frac{1}{2}; \qquad \beta \geqslant \frac{(2(b_F+b_B)+1)(b_F+b_B)}{4b_F-1+(b_F+b_B)(4b_F-2)} \tag{12}$$

and via similar analysis the low-density phase (LD) is present when

$$\alpha < \frac{1}{2} \qquad \text{and} \qquad \beta > \frac{\alpha(b_F+b_B)(1-\alpha+b_F+b_B)}{b_F-\alpha(1-\alpha)+(b_F+b_B)(b_F-\alpha)} \tag{13}$$

and HD is present when

$$\beta < \frac{(2(b_F+b_B)+1)(b_F+b_B)}{4b_F-1+(b_F+b_B)(4b_F-2)} \qquad \text{and} \qquad \beta < \frac{\alpha(b_F+b_B)(1-\alpha+b_F+b_B)}{b_F-\alpha(1-\alpha)+(b_F+b_B)(b_F-\alpha)}, \tag{14}$$

all of which create significant shifts in the phase diagram when b_F and b_B are small. The effect of these changes can clearly be seen in figure 3. The significance of correlations is entirely determined by the relative size of b_F over its minimum value $\left(\frac{1}{4}\right)$. This can be seen by examining the connected part of the correlation function $\langle l_L\chi_b\rangle_c = \langle l_L\chi_b\rangle - \langle l_L\rangle\langle\chi_b\rangle$ which vanishes in the limit $b_F \gg \frac{1}{4}$ independent of the value of b_B and β. This statement is equivalent to saying that an effective out rate can be defined, and that our system collapses onto the diffusable nozzles case.

3.2. Gated entrance

This situation proceeds identically to that above, guided by the particle–hole symmetry that tells us that the system with gated entry with entrance rate α and fixed exit β for a particle is identical to a system for holes with fixed entry alpha and gated exit α. For this reason we will not repeat the results outlined above.

3.3. Gated entrance and exit

The most general situation is algebraically more complex but technically no more difficult. For brevity we quote the boundaries in terms of the predicted value for χ_a and χ_b and we note that $a_F, b_F > \frac{1}{4}$ in all cases. The occupation of the entrance gate χ_a is described by a formula similar to (4) but conditioned on the emptiness of the first lattice site rather than the occupations of the last. We find that where $\alpha \geqslant \frac{1}{2} + \frac{2a_B+\frac{1}{2}}{4a_F-1}$, $\beta \geqslant \frac{1}{2} + \frac{2b_B+\frac{1}{2}}{4b_F-1}$ the system is MC

$$\begin{aligned} J &= \frac{1}{4} \qquad l_1 = 1 - \frac{1}{4\alpha\chi_a} \qquad l_L = \frac{1}{4\beta\chi_b} \\ l_{\text{bulk}} &= \frac{1}{2} \qquad \chi_a = \frac{a_F - \frac{1}{4}}{a_F + a_B} \qquad \chi_b = \frac{b_F - \frac{1}{4}}{b_F + b_B}; \end{aligned} \tag{15}$$

where $\alpha < \frac{1}{2} + \frac{2a_B+\frac{1}{2}}{4a_F-1}$, $\beta > \frac{\alpha(b_f+b_B)\chi_a}{b_F-a_F+(a_f+a_B)\chi_a}$ the system is LD with

$$\begin{aligned} &J = \alpha\chi_a(1-\alpha\chi_a) \qquad l_1 = \alpha\chi_a \qquad l_L = \frac{b_f}{\beta\chi_b} - \frac{b_F+b_b}{\beta} \qquad l_{\text{bulk}} = \alpha\chi_a \\ &\chi_a = \frac{1}{2\alpha^2}\left(\alpha + a_F + a_B - \sqrt{(\alpha+a_F+a_B)^2 - 4\alpha^2 a_F}\right) \qquad \chi_b = \frac{b_F - \alpha\chi_a(1-\alpha\chi_a)}{b_F+b_B} \end{aligned} \tag{16}$$

and where $\beta < \frac{1}{2} + \frac{2b_B+\frac{1}{2}}{4b_F-1}$, $\alpha > \frac{\beta(a_f+a_B)\chi_b}{a_F-b_F+(b_f+b_B)\chi_b}$ the system is HD with

$$\begin{aligned} &J = 1-\beta\chi_b(1-\beta\chi_b) \qquad l_1 = 1 - \frac{\beta\chi_b(1-\beta\chi_b)}{\alpha\chi_a} \qquad l_L = 1-\beta\chi_b \qquad l_{\text{bulk}} = 1-\beta\chi_b \\ &\chi_a = \frac{a_F - \beta\chi_b(1-\beta\chi_b)}{a_F+a_B} \qquad \chi_b = \frac{1}{2\beta^2}\left(\beta + b_F + b_B - \sqrt{(\beta+b_F+b_B)^2 - 4\beta^2 b_F}\right). \end{aligned} \tag{17}$$

Of particular mathematical interest is the invertible algebraic curve predicted as the phase boundary between the LD and the HD phases which is described by

$$\alpha = \frac{\beta(a_f+a_b)\left(\beta + b_F + b_B - \sqrt{(\beta+b_F+b_B)^2 - 4\beta^2 b_F}\right)}{2\beta_2(a_F-b_F) + (b_F+b_b)\left(\beta + b_F + b_B - \sqrt{(\beta+b_F+b_B)^2 - 4\beta^2 b_F}\right)} \tag{18}$$

and results in a curving boundary between phases. The phase diagrams of this curve can be seen in figure 4. Note that this form reverts to a simple straight line when $a_F = b_F$.

The symmetry in the relationship can be easily seen if we express the phase boundary curve as

$$\begin{aligned} &(\beta(\alpha+a_F+a_B) - \alpha(\beta+b_F+b_B))(\beta b_F(\alpha+a_F+a_B) - \alpha a_F(\beta+b_F+b_B)) \\ &\qquad + \alpha^2\beta^2(b_F-a_F)^2 = 0. \end{aligned} \tag{19}$$

4. Monte Carlo simulations

Because of the varying events in the model, it is not possible to use a standard particle picking approach for the MC simulations. Instead we adopt a simple direct method, commonly called the Gillespie algorithm [16], for the simulation. We simulate each choice of α and β such that on average 10^6 hopping events at each site are sampled after a suitable warm-up time. Finite size effects can create significant alterations to the phase diagrams in this type of simulation; we run the bulk of our simulations at $L = 300$ which is sufficiently large for these effects to be suppressed except for close to the phase boundary, where we make use of large systems and larger run-times as required. We determine the phase boundaries by examining

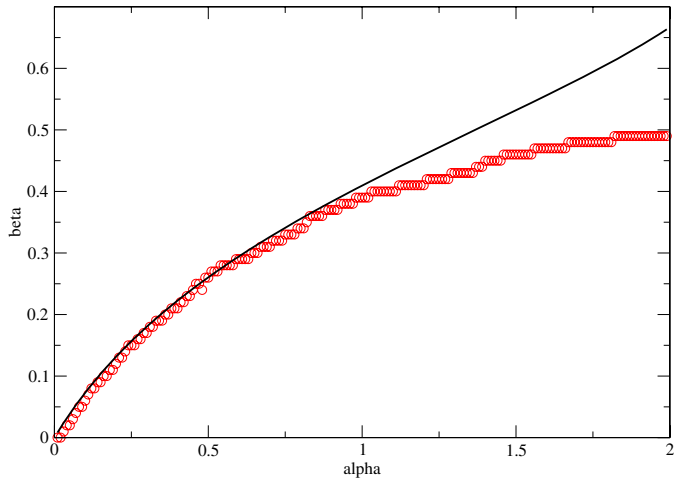

Figure 4. Phase portrait for the double-gated system with $L = 300$. We choose to have the entrance slowly changing ($a_F = 0.4$ and $a_B = 0.2$) and the exit quickly changing ($b_F = 4.0$ and $b_B = 1.0$). The MC phase boundary would begin at the upper-right corner of the plot shown. The plot now diverges from the predicted line in the opposite fashion as shown in figure 3 as the slow rates are on the exit. The qualitative effect of the two gates can be inferred from our earlier analysis of the singly gated system. It is possible that the effect of the slow gate is sufficient to interfere with the behaviour of the other gate, but we have not explored this effect in this study; the effects can be inferred from the singly gated study.

the bulk density which changes discontinuously around the first-order transition between the HD and the LD phases. Where possible this is done in an automated fashion by utilizing the theoretically predicted values for the curves and assessing the best discontinuity between them with a least-squares method augmented with iterative bisection. However, in some cases this is not possible due to the loss of a theoretical description; here the fitting is simply done by hand at evenly spaced points. This method also applies on the second-order boundaries, but is not as clear. We supplement our predictions with reference to the bulk current which continuously asymptotes to $\frac{1}{2}$ in the max current phase.

4.1. Gated out only

We take two examples in this instance, first with values at the exit gate where b_F and b_B are greater than unity, the internal hopping rate, and secondly with b_F and b_B less than unity. The results for these two simulations are shown in figure 2 and figure 3 respectively. The agreement between the theoretical results and the simulated results are excellent in the former case; there are small deviations from the predicted values close to the phase boundary junction. This is due to the increasing rounding off of the discontinuous transition between the bulk densities as the system moves closer to achieving a maximal current phase. Where the rates of exit are slower than the internal transport dynamics, then we have much less good agreement. Here, whilst finite size effects are important, the primary source of disagreement will be due to correlations from the exit conditions penetrating back into the bulk of the system. This can be seen by the accuracy of fit of the improved mean-field case where these correlations are taken into account in a limited fashion. The simulations imply that successive refinements to the MC boundary will result in its disappearance and that only the LD and HD phases actually exist.

In this study we have not gone beyond the simple first step improved mean-field theory; the next iteration involves a cubic equation with significant extra algebraic complexity to produce a closed form analytic solution, even utilizing symbolic computation. Numerical calculation in a similar system has been demonstrated [17] but would not yield the desired result.

4.2. Gated in and gated out

We show a plot of a single example in this case, one with a mix of the conditions utilized above.

This situation gives rise to a more interesting phase diagram with the curved boundary between the low-density and high-density phases and can be seen in figure 4. The fit for small values of α is excellent and follows the predicted curve with high accuracy. The discrepancy due to the correlations now results in the simulated curve dipping below the predicted curve as the entrance gate now has transport rates lower than the bulk. We anticipate that as in the case of a single altered gate the MC phase cannot be maintained.

5. Discussion

We have presented here a simple extension of the asymmetric exclusion process that takes into account exit and entrance rates that are not fixed, but depend on additional transiently binding media that transport the particles on the track away from the confined system. We focused here on describing such a system and computing the phase diagrams with a view that this study is a stepping stone for later studies that may use the information presented here in order to more widely apply the asymmetric exclusion process to transport problems, especially in the biological sciences. There are a host of applications in this area. For example the particles on the track can represent multiple ribosomes in kinetic protein production [2, 3] with rates determined by tRNA abundance. The binding and unbinding rates then represent the chemical attachment process and failure rate at the initiation of the translation process. Alternatively, the particles might represent essential common cellular components such as ATP, electrons or infrastructure proteins that are actively transported and then utilized at the terminus either by a wide set of enzymes or by a specific conformational protein, such as in the construction of bacterial flagellum [18]. Another situation is where the actively transported medium represents an enzyme or similar that consumes a reagent at the terminus. In this case the reagent will be consumed at the exit and in doing so will reduce the rate of 'on' binding, altering the behaviour of the transport system as it proceeds. Not considered here is the potential for non-specific binding of the 'full' receptor (or 'empty' initiator) to the target, off lattice, site which would have the effect of blocking further transport but may have biological significance for some systems.

Acknowledgments

The author would like to thank James Moir for stimulating discussions and Martin Evans for helpful guidance. The author is supported by an RCUK fellowship.

References

[1] Chowdhury D, Schadschneider A and Nishinari K 2005 *Phys. Life. Rev.* doi:10.1016/j.plrev.2005.09.001
[2] Mac Donald J T, Gibbs J H and Pipkin A C 1968 *Biopolymers* **6** 1
[3] Romano M C, Thiel M, Stansfield I and Grebogi C 2009 *Phys. Rev. Lett.* **102** 198104

[4] Evans M R and Sugden K E P 2007 *Phys. A: Stat. Mech. Appl.* **384** 53–8
[5] Blythe R A and Evans M R 2007 *J. Phys. A: Math. Theor.* **40** R333 doi:10.1088/1751-8113/40/46/R01
[6] Derrida B *et al* 1993 *J. Phys. A: Math. Gen.* **26** 1493 doi:10.1088/0305-4470/26/7/011
[7] Derrida B, Domany E and Mukamel D 1992 *J. Stat. Phys.* **69** 667–87
[8] Kolomeisky A B 1998 *J. Phys. A: Math. Gen.* **31** 1153
[9] Janowsky S A and Lebowitz J L 1992 *Phys. Rev.* A **45** 618
[10] Dong J J, Zia R K P and Schmittmann B 2009 *J. Phys. A: Math. Theor.* **42** 015002
[11] Klump S and Lipowsky R 2003 *J. Stat. Phys.* **113** 233
[12] Pronina E and Kolomeisky A B 2005 *J. Stat. Mech.: Theory Exp.* doi:10.1088/1742-5468/2005/07/P07010
[13] Tsekouras K and Kolomeisky A B 2008 *J. Phys. A: Math. Theor.* **41** 465001
[14] Popkov V, Salerno M and Shütz G M 2008 *Phys. Rev.* E **78** 011122
[15] Sugden K E P and Evans M R 2007 *J. Stat. Mech.* P11013
[16] Gillespie D 1976 *J. Comput. Phys.* **22** 403–34
[17] Chou T and Lakatos G 2004 *Phys. Rev. Lett.* **93** 198101
[18] Minamino T, Imada K and Namba K 2008 *Mol. Biosyst.* **4** 1105–15